Common Spatial Patterns for Steady-State Somatosensory Evoked Potentials*

Yunjun Nam[1], Andrzej Cichocki[2] and Seungjin Choi[3]

Abstract— **Steady-state somatosensory evoked potential (SSSEP) is a recently developing brain-computer interface (BCI) paradigm where the brain response to tactile stimulation of a specific frequency is used. Thus far, spatial information was not examined in depth in SSSEP BCI, because frequency information was regarded as the main concern of SSSEP analysis. However, given that the somatosensory cortex areas, each of which correspond to a different body part, are well clustered, we can assume that the spatial information could be beneficial for SSSEP analysis. Based on this assumption, we apply the common spatial pattern (CSP) method, which is the spatial feature extraction method most widely used for the motor imagery BCI paradigm, to SSSEP BCI. Experimental results show that our approach, where two CSP methods are applied to the signal of each frequency band, has a performance improvement from 70% to 75%.**

I. Introduction

The brain computer interface (BCI) is a system that provides a direct communication pathway between the brain and external devices by analyzing various brain signals [1]. Among various BCI techniques, steady-state somatosensory evoked potential (SSSEP) is a paradigm that has been developing recently that use the brain's response to tactile stimulation. The concept of using SSSEP as the medium of the interface was first suggested in [2]. If a single tactile stimulation is given to the subjects, an evoked potential with a specific waveform will be generated. Likewise, if the tactile stimulations are periodically applied in the form of a vibration with a specific frequency, the following evoked potentials will also be periodic. By examining this periodic response with time-frequency analysis, we can detect the type of the stimulation frequency being given to the subject. In their paper, Müller-Putz *et al.* [2] reported that selective attention to a specific stimulus can modulate the induced SSSEP, and they exploited this paradigm to implement a novel BCI system. In their study, two different vibratory stimulations with a frequency range from 20 Hz to 30 Hz were applied on the index finger of the left and the right hand of subjects; then, the system predicted whether the subjects were focusing on the stimulation at the left or right index finger.

To the best of our knowledge, the performance of SSSEP BCI is still too poor to allow for its implementation in a practical interface. To improve the performance, in this study, we apply Fukunaga-Koontz transform-based feature extraction method [3], as applied to the motor imagery-based BCI, which is referred to as "common spatial pattern (CSP)" method [4].

The CSP is one of the most intensively studied feature extraction method for the motor imagery BCI paradigm [5]. The motor imagery paradigm exploits spatial information about activated brain areas. For example, if a subject imagines a left hand movement, the corresponding motor cortex area near C4 (EEG channel located on the right side of the parietal area in the International 10-20 system) is activated, and this activation is observed as the attenuation of the μ-rhythm in the area. Similarly, an imagery right hand movement causes μ-rhythm attenuation in C3 channel, and an imagery foot movement causes the attenuation in Cz channel, and so on. From these spatial differences, CSP finds spatial filters that maximize the difference in the signal power between the two classes to be discriminated. In previous studies, CSP proved its usefulness for extracting a discriminative spatial pattern, outperforming other methods [6], [7].

In the SSSEP-based BCI paradigm, spatial patterns have not been examined in depth, to investigate whether they are crucial for improving BCI performances. In their research, Müller-Putz *et al.* [2] used only three channels (C3, Cz, and C4) along the primary sensorimotor cortex. Dan Zhang [8] used three channels: C3, C4, and one additional channel selected by a statistical test. In both stuides, all the channels contributed equally to the classification procedure, and there were no consideration of spatial correlation between channels.

It should be noted that considering spatial information using a sophisticated feature extraction method could be beneficial for improving the performance of SSSEP BCI. According to the cortical homunculus theory, (see [9], pp. 544−546), the primary somatosensory cortex, which is the main sensory receptive area for tactile stimuli, is located across the central sulcus, as is the primary motor cortex. Two sensory cortices corresponding to the left hand and right hand are located in laterally opposite regions, and the distance between them (11−14 cm according to head size) is sufficient to allow discrimination according to EEG signals. Given that the partial activation of the motor cortex

*This work was supported by National Research Foundation (NRF) of Korea (2012-0005785 and 2012-0005786), POSTECH Rising Star Program, and NRF World Class University Program (R31-10100).

[1]Y. Nam is with the School of Interdisciplinary Bioscience and Bioengineering, Pohang University of Science and Technology, Pohang 790-784, Korea (e-mail: druid@postech.ac.kr)

[2]A. Cichocki is with RIKEN Brain Science Institute, Japan and Systems Research Institute Polish Academy of Science (email: a.cichocki@brain.riken.jp).

[3]S. Choi is with the Department of Computer Science and Engineering and Division of IT Convergence Engineering, Pohang University of Science and Technology, Pohang 790-784, Korea (e-mail: seungjin@postech.ac.kr).

in different areas plays a major role in motor imagery-based BCI, we can assume that analyzing the spatial pattern of somatosensory cortex activation could be beneficial for SSSEP BCI, if selective attention to different body parts can evoke the partial activation of the somatosensory cortex.

Furthermore, the motivation of the CSP is well-suited to SSSEP classification. The objective of CSP is to find the feature vector that can maximize the projected variance of one distribution, while minimizing the variance of another. In the selective attention-based SSSEP BCI, the SSSEP response is observed as an amplitude change in the target frequency. This amplitude is directly related to the variance of the waveform. Therefore, the CSP can extract the optimal filter which can maximize the difference in amplitude responses between the EEG signals from different attention.

Based on the aforementioned assumptions, we applied CSP to SSSEP classification. In their recent research, Ahn *et al.* [10], briefly applied CSP to SSSEP BCI and compared its results with the results of motor imagery BCI. Drawing on their initial approach, in this paper, we evaluate the performance improvement by the CSP, and suggest a modified CSP method suitable for SSSEP classification, which applies two CSP methods, on each frequency band of interest.

The remainder of this paper is organized as follows. In Section II, we describe our experimental design for the SSSEP BCI. In Section III, we describe two CSP-based feature extraction methods for SSSEP classification. In Section IV, the experimental results are presented and the performances of each method are compared. Finally, conclusion is drawn in Section V.

II. Experimental Design

In this section, we will explain the experimental design, including the stimulation unit, EEG recording device, and interface design.

A. SSSEP BCI

An overview of the system is graphically depicted in Fig. 1. To control the transducer, digital control signals with specific frequencies were generated by a C++ based program, and then transmitted through the parallel port. The signals are amplified by the transistor to apply enough power to control the transducer.

The vibratory stimulation was administered by a round shaped-vibration motor with a radius of 1 cm. We present a picture of the transducer attached to a finger in Fig. 2(a). The first transducer was attached on the thumb of the left hand, and the second transducer was attached on the same digit of the right hand using medical tape. During the experiment, the transducer on the left thumb vibrated at 22 Hz, while another transducer on the right thumb vibrated at 27 Hz.

B. EEG Recording

The EEG signals used in this study were recorded using a Biosemi ActiveTwo ® system. The sampling rate was 512 Hz. The montage of the electrodes is depicted by thick circles in Fig. 2(b). The signals in each trial were band-pass filtered between 0.5 Hz and 40 Hz.

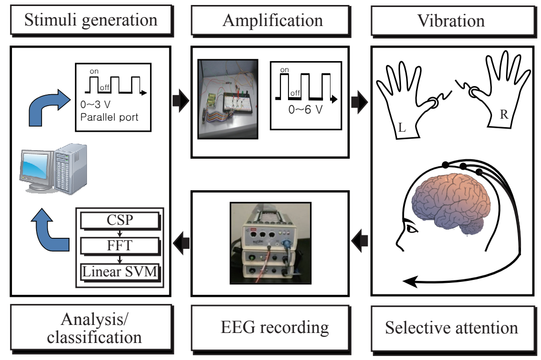

Fig. 1. Overview of the SSSEP-based BCI system

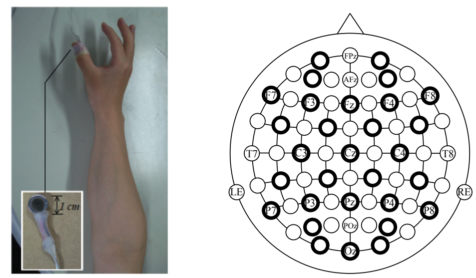

(a) Transducer on finger

(b) EEG channel montage

Fig. 2. Experimental design

C. Interface Design

Based on the implemented system described above, we designed the SSSEP-based interface, which can detect the stimulus on which the subjects are focusing. For each trial, two vibratory stimuli with different frequencies were administered to the subjects, having a duration of 10 s. Before the stimuli were administered, one of the transducers vibrated for 2 s as the cue. The subject was asked to concentrate on the transducer that was indicated by the cue.

For every session, we collected 40 trials, half of which $(n = 20)$ were assigned to the cue on the left hand, and half to the cue on the right hand. The set of trials assigned to the cue on the left hand and right hand are denoted below by $\boldsymbol{L}$ and $\boldsymbol{R}$, respectively. The results of the trials were classified using the methods described in the next section.

III. Method

In this section, we will explain two CSP-based feature extraction methods used for SSSEP classification. The CSP can be integrated with the SSSEP in various ways. For example, CSP can be applied to the raw signals or to the already band-pass filtered signals. To find the optimal method for improving the performance, we designed three different methods, which are briefly schematized in Fig. 3, and compared their performances.

A. Using Amplitudes of Raw Signals (RS)

As the basic approach, for comparison with our proposed methods, we used the amplitudes of the frequencies of the stimuli ($f_1 = 22$ Hz and $f_2 = 27$ Hz) as the feature vector for the classification. Let us denote the mean-centered EEG signals recorded in the n-th trial as $\boldsymbol{X}_n \in \mathbb{R}^{30\times5120}$, while 30 is the number of EEG channels and 5120 is the temporal length of 10 s EEG signals. In this method, the feature vector $\boldsymbol{z}_n$ for $\boldsymbol{X}_n$ is obtained

$$\boldsymbol{z}_n = \begin{bmatrix} \mathrm{Amp}_{(f_1)}(\boldsymbol{X}_n) \\ \mathrm{Amp}_{(f_2)}(\boldsymbol{X}_n) \end{bmatrix}, \tag{1}$$

where $\mathrm{Amp}_{(f)}(\boldsymbol{X})$ is the function that returns the amplitude of FFT (Fast Fourier Transform) on the frequency f from each channel of the signals $\boldsymbol{X}$. In our experiment, the signals from 30-channel EEG sernsors were recorded, and therefore each $\boldsymbol{z}_n$ has the form of $\mathbb{R}^{60\times1}$ vector. To build the classification model to discriminate between $\boldsymbol{z}_{n\in\mathrm{L}}$ and $\boldsymbol{z}_{n\in\mathrm{R}}$, we used a linear support vector machine (SVM). The performance of the classification will be presented in Section IV.

B. CSP on Raw Signals (CSP-R)

As the first step of applying CSP to SSSEP classification, we applied CSP to the raw signals, then compared the amplitudes of extracted signal components.

We calculated two covariance matrices for each class as

$$\begin{aligned} \boldsymbol{\Sigma}_\mathrm{L} &= \frac{1}{N_\mathrm{L}}\sum_{n\in\mathrm{L}} \boldsymbol{X}_n\boldsymbol{X}_n^\top, \quad (2) \\ \boldsymbol{\Sigma}_\mathrm{R} &= \frac{1}{N_\mathrm{R}}\sum_{n\in\mathrm{R}} \boldsymbol{X}_n\boldsymbol{X}_n^\top, \quad (3) \end{aligned}$$

where N_L and N_R are the number of trials in each class. From the sum of two matrices $\boldsymbol{\Sigma} = \boldsymbol{\Sigma}_\mathrm{L} + \boldsymbol{\Sigma}_\mathrm{R}$, we measured the whitening matrix $\boldsymbol{P}$, satisfying $\boldsymbol{P}^\top\boldsymbol{\Sigma}\boldsymbol{P} = \boldsymbol{I}$. If the eigen-decomposition of $\boldsymbol{\Sigma}$ has the form $\boldsymbol{\Sigma} = \boldsymbol{U\Lambda U}^\top$, the whitening matrix $\boldsymbol{P}$ can be measured by $\boldsymbol{P} = \boldsymbol{U\Lambda}^{-\frac{1}{2}}$.

Let us consider $\boldsymbol{V}$ that can diagonalize $\boldsymbol{P}^\top\boldsymbol{\Sigma}_\mathrm{L}\boldsymbol{P}$. Rewrite $\boldsymbol{P}^\top\boldsymbol{\Sigma}\boldsymbol{P} = \boldsymbol{I}$ to $\boldsymbol{P}^\top(\boldsymbol{\Sigma}_\mathrm{L} + \boldsymbol{\Sigma}_\mathrm{R})\boldsymbol{P} = \boldsymbol{I}$, and apply $\boldsymbol{V}$ to both sides of the equation as

$$\boldsymbol{V}^\top(\boldsymbol{P}^\top\boldsymbol{\Sigma}_\mathrm{L}\boldsymbol{P} + \boldsymbol{P}^\top\boldsymbol{\Sigma}_\mathrm{R}\boldsymbol{P})\boldsymbol{V} = \boldsymbol{I}. \tag{4}$$

With considering that both of $\boldsymbol{V}^\top(\boldsymbol{P}^\top\boldsymbol{\Sigma}_\mathrm{L}\boldsymbol{P})\boldsymbol{V}$ and $\boldsymbol{V}^\top(\boldsymbol{P}^\top\boldsymbol{\Sigma}_\mathrm{R}\boldsymbol{P})\boldsymbol{V}$ are diagonal matrices, the spatial filter matrix $\boldsymbol{W} = \boldsymbol{PV}$ can diagonalize $\boldsymbol{\Sigma}_\mathrm{L}$ and $\boldsymbol{\Sigma}_\mathrm{R}$ simultaneously. Meanwhile, if i-th diagonal element of $\boldsymbol{W}^\top\boldsymbol{\Sigma}_\mathrm{L}\boldsymbol{W}$ is λ_i, the i-th diagonal element of $\boldsymbol{W}^\top\boldsymbol{\Sigma}_\mathrm{R}\boldsymbol{W}$ should be $1-\lambda_i$. $\boldsymbol{W}$ can diagonalize both of $\boldsymbol{\Sigma}_\mathrm{L}$ and $\boldsymbol{\Sigma}_\mathrm{R}$, and corresponding diagonal values are reversely ordered. Therefore, a spatial filter $\boldsymbol{w}_i$ (i-th column vector of $\boldsymbol{W}$) associated with larger λ_i close to 1, can maximize the variance of the projected signals of $\boldsymbol{X}_{n\in\mathrm{L}}$, while minimize the variance of the projected signals of $\boldsymbol{X}_{n\in\mathrm{R}}$.

To extract the discriminative feature, which can maximize the difference in signal power between two classes, we collected $\boldsymbol{w}_i$ corresponding to the four largest and four smallest λ_i, and denoted them by

$$\tilde{\boldsymbol{W}} = [\boldsymbol{w}_1, \cdots, \boldsymbol{w}_4, \boldsymbol{w}_{27}, \cdots, \boldsymbol{w}_{30}], \tag{5}$$

for use as the projection vectors. Finally, the feature vector $\boldsymbol{z}'_n \in \mathbb{R}^{16\times1}$, corresponding to the n-th trial $\boldsymbol{X}_n$ was measured by

$$\boldsymbol{z}'_n = \begin{bmatrix} \mathrm{Amp}_{(f_1)}(\tilde{\boldsymbol{W}}^\top\boldsymbol{X}_n) \\ \mathrm{Amp}_{(f_2)}(\tilde{\boldsymbol{W}}^\top\boldsymbol{X}_n) \end{bmatrix}. \tag{6}$$

$\boldsymbol{z}'_n$ represents the amplitudes on f_1 and f_2 of the extracted signal components.

C. CSP on Filtered Signals (CSP-F)

In the previous CSP-R approach, we applied CSP to the raw signals, then measured the amplitudes from the extracted signal components. However, the SSSEP analysis exploits the signals of two frequency bands. To extract better spatial filters, which work more efficiently for each frequency band, we applied CSP method to already band-pass filtered signals for two frequency bands, respectively. We first obtained band-pass filtered signals $\boldsymbol{X}_{n(f_1)}$ and $\boldsymbol{X}_{n(f_2)}$ from the raw signals $\boldsymbol{X}_n$. $\boldsymbol{X}_{n(f_1)}$ is band-pass filtered between $f_1 - 1$ Hz to $f_1 + 1$ Hz, and $\boldsymbol{X}_{n(f_2)}$ is filtered between $f_2 - 1$ Hz to $f_2 + 1$ Hz,

We calculated the covariance matrices $\boldsymbol{\Sigma}_{\mathrm{L}(f_1)}$ and $\boldsymbol{\Sigma}_{\mathrm{R}(f_1)}$ from $\boldsymbol{X}_{(n\in\mathrm{L})(f_1)}$ and $\boldsymbol{X}_{(n\in\mathrm{R})(f_1)}$, and calculated $\boldsymbol{\Sigma}_{\mathrm{L}(f_2)}$ and $\boldsymbol{\Sigma}_{\mathrm{R}(f_2)}$ from $\boldsymbol{X}_{(n\in\mathrm{L})(f_2)}$ and $\boldsymbol{X}_{(n\in\mathrm{R})(f_2)}$, as we did in (2) and (3). By the CSP approach, already described in III-B, we obtained the spatial filter matrices $\boldsymbol{Q}$ and $\boldsymbol{R}$. $\boldsymbol{Q}$ can diagonalize $\boldsymbol{\Sigma}_{\mathrm{L}(f_1)}$ and $\boldsymbol{\Sigma}_{\mathrm{R}(f_1)}$ simultaneously, while $\boldsymbol{R}$ can diagonalize $\boldsymbol{\Sigma}_{\mathrm{L}(f_2)}$ and $\boldsymbol{\Sigma}_{\mathrm{R}(f_2)}$.

From $\boldsymbol{Q}$ and $\boldsymbol{R}$, we collected the eigenvectors corresponding to the four largest and four smallest eigenvalues and denoted them by

$$\begin{aligned} \tilde{\boldsymbol{Q}} &= [\boldsymbol{q}_1, \cdots, \boldsymbol{q}_4, \boldsymbol{q}_{27}, \cdots, \boldsymbol{q}_{30}], \quad (7) \\ \tilde{\boldsymbol{R}} &= [\boldsymbol{r}_1, \cdots, \boldsymbol{r}_4, \boldsymbol{r}_{27}, \cdots, \boldsymbol{r}_{30}]. \quad (8) \end{aligned}$$

$\tilde{\boldsymbol{Q}}$ is the discriminative filter for $\boldsymbol{X}_{n(f_1)}$, while $\tilde{\boldsymbol{R}}$ is the filter for $\boldsymbol{X}_{n(f_2)}$. Therefore, we measured the amplitude of $\tilde{\boldsymbol{Q}}^\top\boldsymbol{X}_{n(f_1)}$ on f_1 Hz, and the amplitude of $\tilde{\boldsymbol{R}}^\top\boldsymbol{X}_{n(f_2)}$ on f_2 Hz. By concatenating the amplitudes, we obtained the feature vector $\boldsymbol{z}''_n \in \mathbb{R}^{16\times1}$ corresponding to $\boldsymbol{X}_n$:

$$\boldsymbol{z}''_n = \begin{bmatrix} \mathrm{Amp}_{(f_1)}(\tilde{\boldsymbol{Q}}^\top\boldsymbol{X}_{n(f_1)}) \\ \mathrm{Amp}_{(f_2)}(\tilde{\boldsymbol{R}}^\top\boldsymbol{X}_{n(f_2)}) \end{bmatrix}. \tag{9}$$

Then, the classification model for discriminating $\boldsymbol{z}''_{n\in\mathrm{L}}$ and $\boldsymbol{z}''_{n\in\mathrm{R}}$ was trained.

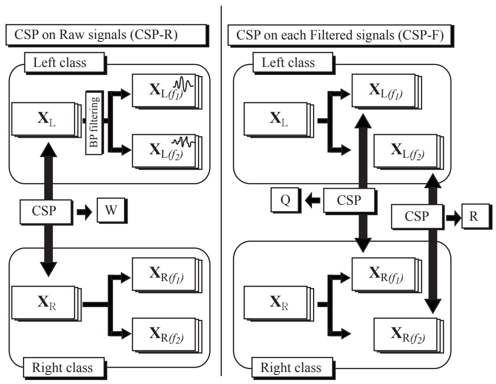

Fig. 3. Two methods for applying the CSP for the SSSEP classification

Subjects	Sessions	RS	CSP-R	CSP-F
1	1	60.0	62.5	**85.0**
	2	72.5	47.5	**80.0**
2	1	62.5	57.5	**77.5**
	2	**87.5**	80.0	70.0
3	1	57.5	42.5	**62.5**
	2	**87.5**	57.5	80.0
4	1	62.5	52.5	**72.5**
mean		70.0	57.1	**75.4**

TABLE I
CLASSIFICATION ACCURACY

IV. EXPERIMENTS

Using the three methods described in the previous section (RS, CSP-R, and CSP-F), we obtained three kinds of feature values ($\boldsymbol{z}$, $\boldsymbol{z}'$, and $\boldsymbol{z}''$). We classified the obtained feature values by applying linear SVM [11], and compared the results of five-fold cross-validation.

For the experiment, the signals are recorded from four healthy male subjects, whose ages varied from 26 to 29 years (mean value = 27.8). The performances are presented in Table I. The result of one session of Subject 4 is omitted, because all performances could not reach 60%. As shown in the table, in most of cases, the CSP-F method outperformed RS and CSP-R.

In Fig. 4, we plot the exemplary spatial patterns, obtained from the column vectors of $(\boldsymbol{W}^{-1})^\top$, $(\boldsymbol{Q}^{-1})^\top$, and $(\boldsymbol{R}^{-1})^\top$, to examine their correspondence to the neurophysiological background. The spatial patterns from $(\boldsymbol{Q}^{-1})^\top$ and $(\boldsymbol{R}^{-1})^\top$, obtained from the CSP-F method, showed more meaningful results than the patterns from CSP-R method. $(\boldsymbol{Q}^{-1})_4^\top$, meaning the fourth column vector of $(\boldsymbol{Q}^{-1})^\top$ emphasized the parietal area corresponding to the somatosensory cortex. $(\boldsymbol{Q}^{-1})_{28}^\top$ and $(\boldsymbol{R}^{-1})_2^\top$ showed laterally antisymmetric patterns. These patterns can represent desynchronization between the somatosensory cortices of the left and right hemispheres. We believe that CSP can serve an important role in improving the performance of SSSEP BCI, by considering the spatial information more sophisticatedly, as shown in the results.

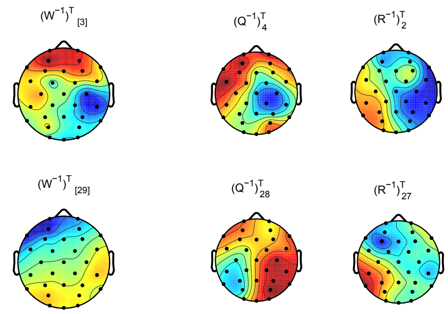

(a) CSP-R (b) CSP-F

Fig. 4. Spatial patterns from each method

V. CONCLUSIONS

In this paper we have applied the CSP method to SSSEP BCI to investigate wheter considering spatial information is beneficial for SSSEP analysis. We described the potential of CSP for improving the performance of SSSEP BCI, and also described the implementation procedure. From the experimental results, CSP-F method, in which two CSP methods are applied to each frequency band, showed a performance improvement from 70.0% to 75.4%. In our future work, we will perform additional investigations to verify the exact spatial pattern of SSSEP, which we believe are essential considerations for realizing practical SSSEP BCI.

REFERENCES

[1] J. R. Wolpaw, N. Birbaumer, D. J. McFarland, G. Pfurtscheller, and T. M. Vaughan, "Brain-computer interfaces for communication and control," *Clinical Neurophysiology*, vol. 113, pp. 767–791, 2002.

[2] G. R. Müller-Putz, R. Scherer, and G. Pfurtscheller, "Steady-state somatosensory evoked potentials: Suitable brain signals for brain computer interfaces?" *IEEE Transactions on Neural Systems and Rehabilitation Engineering*, vol. 14, pp. 30–37, 2006.

[3] K. Fukunaga and W. L. G. Koontz, "Application of the Karhunen-Loève expansion to feature selection and ordering," *IEEE Transactions on Computers*, vol. 19, no. 4, pp. 311–318, 1970.

[4] J. Müller-Gerking, G. Pfurtscheller, and H. Flyvbjerg, "Designing optimal spatial filters for single-trial EEG classification in a movement task," *Clinical Neurophysiology*, vol. 110, pp. 787–798, 1999.

[5] B. Blankertz, R. Tomioka, S. Lemm, M. Kawanabe, and K. R. Müller, "Optimizing spatial filters for robust EEG single-trial analysis," *IEEE Signal Processing Magazine*, pp. 41–56, January 2008.

[6] B. Blankertz, K. R. Müller, D. J. Krusierski, G. Schalk, J. R. Wolpaw, A. Schlögl, G. Pfurtscheller, and N. Birbaumer, "The BCI competition III: Validating alternative approaches to actual BCI problems," *IEEE Transactions on Neural Systems and Rehabilitation Engineering*, vol. 14, pp. 153–159, 2006.

[7] M. Tangermann, K.-R. Müller, A. Aertsen, N. Birbaumer, C. Braun, C. Brunner, R. Leeb, C. Mehring, K. J. Miller, G. Müller-Putz, G. Nolte, G. Pfurtscheller, H. Preissl, G. Schalk, A. Schlögl, C. Vidaurre, S. Waldert, and B. Blankertz, "Review of the BCI competition IV," *Frontiers in Neuroscience*, vol. 6, no. 55, 2012.

[8] D. Zhang, Y. Wang, A. Maye, A. K. Engel, X. Gao, B. Hong, and S. Gao, "A brain-computer interface based on multi-modal attention," in *Proceedings of IEEE EMBS Conference on Neural Engineering*, Kohala Coast, Hawaii, 2007, pp. 414–417.

[9] K. S. Saladin, *Anatomy and Physiology: The Unity of Form and Function*, 4th ed. McGraw-Hill, 2007.

[10] S. Ahn and S. C. Jun, "Feasibility of hybrid BCI using ERD- and SSSEP- BCI," in *International Conference on Control, Automation and Systems*, Jeju Island, Korea, 2012, pp. 2053–2056.

[11] C. Chang and C. Lin, "LIBSVM: A library for support vector machines," *ACM Transactions on Intelligent Systems and Technology*, vol. 2, pp. 27:1–27:27, 2011.